

Determination of Cortisol Hormone from Sweat Samples and Interpretation with Microcontroller

Muhammed Ertuğrul ÇAPAN^{1*}, Ebru CİNGÖZ ÇAPAN², Hasan Uğur ÖNCEL³, Ercan ARICAN⁴

¹ *Istanbul Gedik University, Faculty of Health Sciences, Department of Occupational Health and Safety, 34913, Istanbul, Turkey*¹

^{2,4} *Istanbul University, Faculty of Arts and Sciences, Department of Molecular Biology and Genetics, 34134, İstanbul, Turkey*

³ *Istanbul Gedik University, Faculty of Health Sciences, Department of Nutrition and Dietetics, 34913, Istanbul, Turkey*



(ORCID: [0000-0001-9398-7171](https://orcid.org/0000-0001-9398-7171))²(ORCID: [0000-0002-5296-0009](https://orcid.org/0000-0002-5296-0009))

(ORCID: [0000-0002-6900-1955](https://orcid.org/0000-0002-6900-1955)) (ORCID: [0000-0002-1676-5919](https://orcid.org/0000-0002-1676-5919))

Keywords:

Microfluidic, Cortisol, Hormone, Microcontrollers, Colorimetric Analysis.

Abstract

Cortisol, the body's stress hormone, regulates metabolism and the immune system. It also affects various body systems, such as the cardiovascular, respiratory, reproductive, and musculoskeletal systems. This study aims to quantitatively analyze cortisol hormone levels using colorimetric analysis with microcontrollers. The research focuses on detecting cortisol from artificial sweat samples utilizing microfluidic layers and microcontroller systems. This system employs an ESP 32 microcontroller within a closed environment, where the color changes on the microfluidic layer are photographed and quantified in terms of cortisol levels (ug/mL) based on RGB values obtained through basic image processing algorithms. The blue tetrazolium method used in the colorimetric analysis provides stable color changes and is preferred for its rapid reaction time (10 minutes). The system yields precise and reliable results with low detection limits (0.3 ug/mL), demonstrating high analytical performance. With the integration of the ESP 32 Cam module, the system can accurately measure cortisol levels across a wide concentration range (0.8 – 60 ug/mL). This technological approach leverages the advantages of wearable technologies in the field of biomedical engineering, enabling continuous monitoring of cortisol levels and facilitating the clinical assessment of these data.

1. Introduction

For organisms to perform vital functions and respond to internal or external changes, systems need to be in constant communication. This communication occurs through two pathways: the nervous system and the hormonal system. While the nervous system enables rapid information transmission, hormonal changes involve a slower process, including stages such as hormone production, secretion, and transportation.

Molecules produced by endocrine glands such as the pituitary gland, thyroid gland, parathyroid glands, adrenal glands, gonads (ovaries and testes),

pancreas, and hypothalamus are defined as hormones. Hormones regulate metabolism, growth and development, the composition of body fluids, and reproductive systems. Endocrine refers to the release of products from various glands into the bloodstream in response to specific stimuli. Hormones entering the bloodstream are transported to target cells. Hormones can affect specific target cells as well as different cell types. This effect is defined by interactions with molecules located on or within the target cell, triggering biochemical processes that can alter the activity or function of the target cell. These processes are capable of changing the activity or function of the

* Corresponding author: ertugrulcapann@gmail.com

Received:18.04.2024, Accepted:02.09.2024

target cell [1]. Hormone analysis holds significant importance, particularly in the fields of biology and medicine, for detecting syndromes, diseases, and emerging anomalies. Hormone analysis is frequently relied upon for identifying disorders and abnormalities. With advancing technology, various methods for hormone analysis have emerged, each with its own advantages and disadvantages. Not all hormones can be detected in the same manner, as the differences among hormones have led to the development of different detection methods [2]. Cortisol hormone is the primary glucocorticoid secreted from the adrenal cortex, influencing different functions in various systems of the body. Its secretion is regulated within the Hypothalamus-Pituitary-Adrenal axis, and potential dysregulation can lead to Cushing's syndrome or Addison's disease. Additionally, cortisol is considered a stress hormone in organisms, with effects on metabolism regulation, inflammatory response, immunity, respiration, and the reproductive system.

For these reasons, measuring and monitoring cortisol levels is highly important. Cortisol levels can be measured from body fluids such as blood, saliva, and sweat, and also from hair and nails. Human sweat and saliva fluids have comparable cortisol levels. While enzyme-linked immunosorbent assay (ELISA) testing is the gold standard for cortisol analysis, various successful methods for cortisol hormone measurement have been described in the literature.

The amount of cortisol hormone can be determined using chromatography, immunoassays, and electrochemical immuno-detection methods [3]. While commonly used methods allow for high-accuracy analysis, they often require large sample volumes, lengthy testing periods, specialized equipment, and experienced personnel, making many identified analyses unsuitable for general use. Microfluidics are analytical devices composed of cellulose-based papers, eliminating the need for extra fluid pumps, and consisting of absorbent papers/membranes. These layers enable analyses, especially on fluids, such as antigen-antibody detections and colorimetric analyses. Microfluidics devices are cost-effective, portable, flexible, lightweight, and can be integrated into different systems. The fundamental working principle involves the absorption of analysis reagents into the absorbent layer and the creation of channels for fluid transfer and transportation.

Wearable devices belong to the category of electronic devices that can be worn as accessories, embedded in clothing, implanted into the user's body, and even applied as tattoos. These devices, supported by microprocessors and equipped with data

transmission and reception capabilities over the Internet, have practical applications [4].

These devices play a crucial role in personalized medicine as they can continuously collect data from the human body over time to detect meaningful changes in health status for preventive intervention purposes. A flexible electronic device typically includes several key components, including a substrate, an active layer, and an interface layer. In this context, detection methods with high mobility, flexibility, and adaptability provide a natural interaction between electronics and the human body, owing to their unique features [5].

Microcontrollers are embedded systems that control the actions and features of a device while it is in operation [6]-[7]. Most of the time, they control a specific task in the device rather than all functions of the device; they contain both software and hardware components [8]. Microcontrollers are commonly known today as single-board computers, popularly referred to as microcomputers [9]-[10].

However, microcontrollers should not be confused with microprocessors used for general-purpose computing; microcontrollers are designed for specific purposes [11]. The aim of this study is to contribute to biotechnology-based research by enabling the real-time detection of cortisol hormone using a practical, wearable device. Colorimetric detection methods are particularly prominent in biotechnological approaches and wearable technology due to their quick results, high accuracy, and low cost of production/utilization. Literature reviews indicate that wearable technology and colorimetric methods are often used together, but it has been observed that transporting color changes for analysis is not feasible. In this study, our primary goal was to create portable devices. Additionally, the lack of reusability in previously designed systems and the need for continuous bulk changes, including sensors, are also disadvantages. Making the wearable device reusable increases the usability of the system.

The developed system focuses on establishing a connection via the web between the wearable microfluidic-based device and a reading area, allowing measurements to be taken from the web. Furthermore, by storing the measurements taken from the wearable device within the web, the system aims to enable users to track changes in cortisol hormone levels. Thus, the system aims to contribute to the development of systems that enable low-cost, rapid detection, continuous monitoring of tested parameters, and analysis of results obtained at advanced stages.

In the conducted studies, the analysis of cortisol hormone was performed through colorimetric

color changes on a microfluidic layer. The resulting color changes were interpreted and quantitatively determined through a hardware-integrated system with a camera in the wearable device.

2. Material and Method

Hydrocortisone acetate (Sigma 5003-3), tetramethylammonium hydroxide (Sigma 7559-2), methanol (99% ACS grade), and blue tetrazolium (Sigma 1871223), No. 4 Whatman paper, No. 1 Whatmann Chromatography paper, Thin Layer Chromatography paper, Whatmann Glass Microfiber Filter paper, Coarse Filter Paper, Cotton-Based Sweat Absorbent Pad agar, glycerin, Tween 20, ESP 32 Cam, FTDI, Mini USB B cable, breadboard, jumper cable, 18*10*8 cm PVC box.

2.1. Preparation of Cortisol Stock Solution

Cortisol stock solutions were freshly prepared weekly using hydrocortisone acetate and ethanol.

2.2. Blue Tetrazolium Method

A 5% w/v tetramethylammonium hydroxide solution is prepared by diluting 5 mL of the aqueous solution in 45 mL of methanol. A second solution containing 100 mg of blue tetrazolium dissolved in 50 mL of methanol is prepared. Both solutions are mixed in equal proportions. Stored at room temperature.

2.3. Agar-Based Hydrophobization with Thermoplastic

In this method, the effect of hydrophobization by freezing the agar-based viscous liquid on paper was investigated, and described as thermoplastic in the literature. For this, 0.25 g of Agar agar was mixed with 10 mL of water and 1.5 mL of glycerin until boiling. Before reaching room temperature, 1 mL of Tween 20 was added and applied to the cut filter papers by melting. In this way, one surface of the microfluidic is hydrophobized.

2.4. Water Contact Angle

The water contact angle technique is used to determine the hydrophobicity or hydrophilicity of the surface. Water droplets tend to spread on hydrophilic surfaces, but on hydrophobic surfaces, droplets tend to form spherical shapes instead of spreading and being absorbed. A surface on which water is wetted (contact angle less than 90 degrees) is called a hydrophilic surface, while a surface not wetted by

water (contact angle greater than 90 degrees) is called a hydrophobic surface. After the experiments, the water contact angles formed by liquids colored with food dye were determined on filter papers using various hydrophobization methods.

2.5. Sweat Absorbent Region Studies

The purpose of the sweat absorbent region is to collect sweat formed on the skin by creating a large surface and transferring it to the sample application area of the microfluidic layer. Therefore, liquid retention should be high. In the study, based on the absorbency capacities of the selected papers as the reaction zone, the amount of sample to be collected from the user needs to be taken into account to select the sweat absorbent region.

2.6. Artificial Sweat Sample Studies

Artificial sweat solutions were prepared to be both alkaline and acidic. For the alkaline artificial sweat solution, 0.05 g L-Histidine monohydrochloride and 0.5 g Disodium hydrogen phosphate were dissolved in 100 ml of distilled water. The pH was adjusted to 8 using NaOH.

The acidic artificial sweat solution was prepared by dissolving 0.05 g L-Histidine monohydrochloride, 0.5 g NaCl, and 0.22 g Sodium dihydrogen phosphate in 100 ml of distilled water. The pH was adjusted to 5.5 using NaOH. From the prepared sweat samples, 200 uL was transferred to separate Eppendorf tubes. Then, hydrocortisone solution (h:h) was added to each tube sequentially to achieve concentrations of 60, 40, 10, 5, 2, and 1 ug/mL.

2.7. Microcontroller Studies

In the study, it is possible to divide the setup and programming of technology-related components into 2 stages. Firstly, the connection of the Esp 32 Cam development board was made using the FTDI programming board, and it was programmed in C language using the Esp 32, ESPAsync Web, Async TCP libraries in the Arduino IDE. At the end of the study, the control of the board was provided via the web server. Thus, by using the buttons on the web interface, images were taken and transferred to the Firebase platform, which provides real-time database service. In the second stage, the Python programming language, Open Cv and NumPy libraries, and the firebase-admin package, which connects to the Python-Firebase platforms, were used. Numerical operations were performed on the image obtained

from Firebase, and the results were printed on the result screen.

2.7.1. Connection and Programming of Esp 32 Cam Development Board

Throughout the study, a Monster Abra A.5 V18.2 (Windows 10) model computer was used for all

programming processes. The connection between the development board and the computer was made using the FTDI card, as shown in Figure.1. For the connection between the boards, a breadboard and male-to-male jumper cables were used. The Mini USB B cable attached to the FTDI card was connected to the computer (Figure 1).

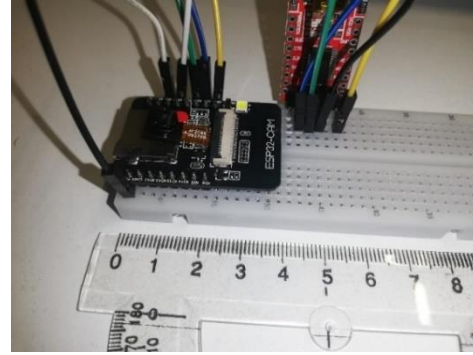
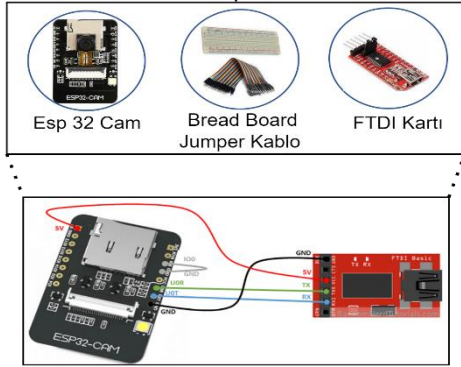


Figure 1. Schematic diagram showing the necessary components for the connection of the ESP 32 Cam development board.

Arduino IDE version 2.0.2 was downloaded from the website "https://www.arduino.cc/en/software". After the installation was completed, for the installation of the Esp 32 library, the "Preferences" menu was opened from the "File" menu at the top left of the Arduino IDE, and the link "https://dl.espressif.com/dl/package_esp32_index.json" was added to the "Additional Board Manager URLs" section, and the "OK" button at the bottom right was clicked. After the installation of the board was completed, the "Tools" menu was selected again, and the "AI Thinker ESP32 CAM" board was selected from the "Board" section. The library installation is completed.

Initially, programming was carried out for taking photos with ESP 32. In the scope of the study, code sources shared by Rui Santos at <https://randomnerdtutorials.com/> were used. For the transfer of the photo taken with the ESP 32 Cam development board to the Firebase database platform, code sources shared by Sara Santos at <https://randomnerdtutorials.com/> were utilized.

2.7.2. Designing the Result Screen

In this stage of the study, obtaining the image from the Firebase platform, performing the operations, and conveying the result value to the user were realized. Firstly, the Scientific Python Development Environment Spyder (5.1.5) IDE was installed on the computer, and the work was started. Python version 3.11.0 was used.

Spyder IDE was used for Python programming. In the Python program, the connection of the application with the Firebase database was established. The region to be analyzed in the received image was cropped, and the average R, G, B channel intensities of the cropped region and the Z-Score value from these values were calculated.

Each image was acquired using the OpenCV library, ensuring consistent imaging conditions across all samples. A fixed region of interest (ROI) was selected from each image, and this area was consistently cropped for analysis. The coordinates defining the ROI (x1, y1, x2, y2) were kept constant for all images to ensure comparability. For each image, the designated ROI was cropped. This region, represented as a specific rectangular area within the image, allowed for a controlled analysis of color

changes. The chosen coordinates ensured that the same area was analyzed across all samples. The RGB values of each pixel within the cropped ROI were extracted, and the average RGB value for the entire region was then calculated using the following formula for each channel

$$(R, G, B): R_{\text{average}} = \frac{1}{N} \sum R_i, \quad (1)$$

$$G_{\text{average}} = \frac{1}{N} \sum G_i, \quad (2)$$

$$B_{\text{average}} = \frac{1}{N} \sum B_i. \quad (3)$$

Here, N represents the total number of pixels within the ROI, while R_i , G_i and B_i denote the RGB values of each individual pixel.

The application of this method enabled the consistent tracking of color changes within the defined ROI across all images. The average RGB values provided a reliable metric for comparing different samples. By maintaining fixed imaging conditions (illumination source, light intensity, and distance), the applicability of the algorithm was validated, negating the need for alternative image processing methods.

The results obtained from 10 repetitions for each concentration were classified according to the result value to create label value ranges. Finally, control trials were conducted, and the study was completed.

2.7.3. Design of the Image Capture Box

To create stability in the photo to be taken, a shooting box was used to create a constant light intensity and a constant distance (Figure 2). It was determined that the development board captured the photo from a distance of 10 cm with the best clarity. Therefore, a box design was made with a distance of 10 cm between the board and the microfluidic. The dimensions of the image capture box are 18x10x8 cm.

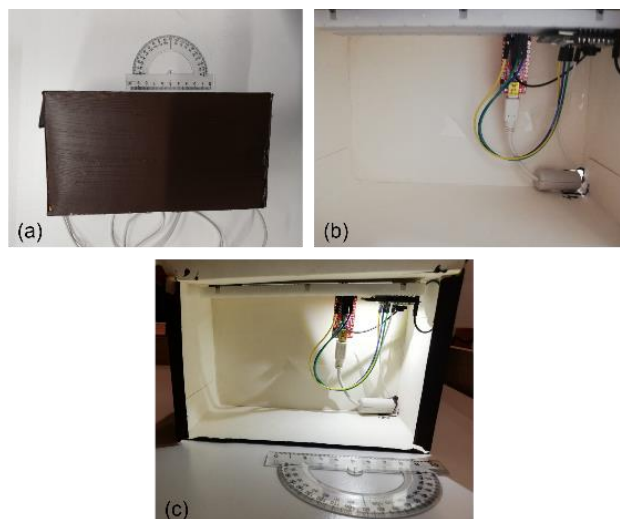


Figure 2. Shooting box, (a) External view of the image capture box, (b) Placement of the microcontroller/development board inside the box, (c) Diagram showing the microcontroller/development board in working condition.

3. Results

3.1. Methylene Blue Method

The relevant method was initially evaluated in Eppendorf tubes. At this stage, 100 μL of tetramethylammonium hydroxide and 100 μL of methylene blue solution were added to the tube and vortexed. Then, cortisol stock at appropriate concentrations was added and vortexed again. The reaction reached equilibrium after 10 minutes. The colors obtained from the reaction are shown in Figure 3.



Figure 3. Color scale obtained after the reaction of stocks containing cortisol at concentrations of 60, 50, 40, 30, 20, 10, 5, 2, 1, 0.8, 0.4, and 0.2 $\mu\text{L}/\text{mL}$ with the appropriate proportions of the color reagent.

3.2. Hydrophobization with Agar-Based Thermoplastic

Agar-based thermoplastic applied to cut filter papers rapidly solidified through the melting method. Colored water was applied to the agar-applied paper (Figure 4). This method enabled one-way hydrophobization.

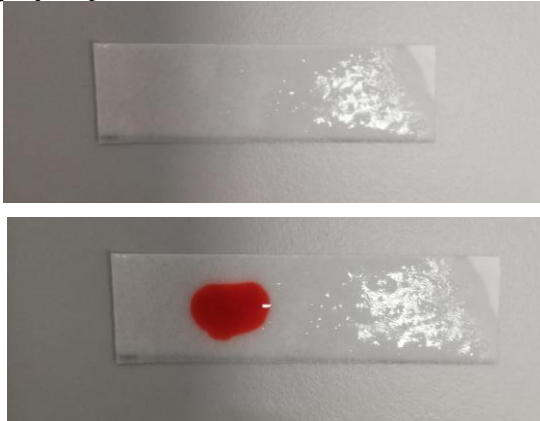


Figure 4. Figure showing the results of hydrophobization using the thermoplastic method.

3.3. Sweat Absorption Zone Studies

The liquid absorption capacities of the selected papers were calculated in the study. The results of the study are provided in Table 3.1.

Table 3.1: Table showing the liquid absorption capacities of the selected papers.

Absorbent Region	Capacity (μL)
No. 4 Whatman paper	40
No. 1 Whatman Chromatography paper	42
Thin Layer Chromatography paper	38
Whatman Glass Microfiber Filter paper	35
Coarse Filter Paper	30
Cotton-based Sweat Absorbent Pad	50

3.4. Microfluidic Arrangement

In the scope of the study, the cellulose-based microfluidic design included thick filter paper, No. 3

Whatman paper, No. 4 Whatman paper, and CHR 1 Whatman chromatography paper.

With the designed system, sweat samples collected from the user will be gathered via the wearable microfluidic layer. The microfluidic layer will be removed, immersed in the reactive solution contained in the created kit, and left to stand for 10 minutes. After the waiting period, discoloration will occur in the area where sweat samples are collected within the microfluidic, and the R (red), G (green), B (blue) channel density values will be analyzed with microcontrollers. Data will be shared with the user through a computer application created.

The created microfluidics were applied with 60 μL of solutions with different cortisol concentrations prepared with pure water to the sweat collection areas and left to stand for 15 minutes to ensure transfer to the sampling area. After 15 minutes, the microfluidics were immersed in the prepared liquid reagent in Eppendorf tubes and photographed after 10 minutes. The color change is shown in Figure 5.



Figure 5 The figure demonstrating the color reaction of the designed system with cortisol concentrations of 50, 40, 30, 20, 10, 5, 2, 1, 0.8, and 0.4 $\mu\text{g}/\text{mL}$, respectively.

3.5. Microcontroller Studies

The Esp32 development board was connected to the computer via USB cable through FTDI, and it was observed that the Esp32 development board was functioning properly from the serial port screen of the Arduino IDE.

During the program setup, the access address generated on the Serial Port Screen was entered into the web browser to run. The interface opened after this connection is completed is shown. When the "Capture Image" button is selected from the interface, the Esp32 development board inside the box captures the image, and the capture date, name, file format, and size of the image are stored in temporary memory. If no action is taken at this stage, the working page is closed, or a new image is captured, the saved image is deleted. If the "Show Image" button is selected, the image temporarily stored is shown to the user. If the user finds the

captured image suitable for use, they select the "Send" button, and the data stored in temporary memory is directed to the Firebase platform (Figure 6). The image and related information were sent to the Firebase platform.



Figure 6 Interface allowing control of the Esp32 development board via the web server and the captured image.

Images captured from the Esp32 development board cannot be directly saved to the storage units on the computer but can be transferred either to a separate storage unit via an SD card or to a web server via the Wi-Fi connection port. For this reason, in this study, a Python program was used to save the captured image on the computer, select the regions to be analyzed, determine the intensity of the R, G, and B channels, and determine the z-score values. The regions for analysis from the raw image obtained from the Firebase platform are shown in Figure 7. The average channel intensity and z-score value in Roi1 are shown in Figure 7.

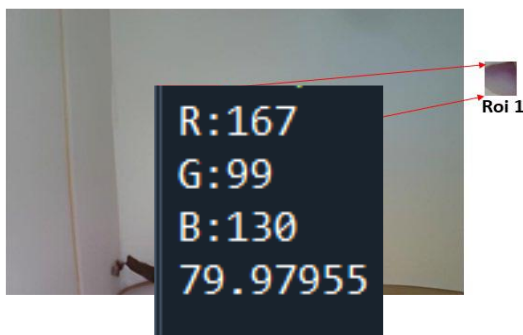


Figure 7 Image of the region of interest (ROI1) to be analyzed (a). Image showing the average RGB value and Z-score of Roi1 displayed on the Spyder console screen (b).

3.6. Validation Studies

The relevant system was tested in 10 repetitions, and the RGB values of the reaction regions were captured using a closed system and a microcontroller-based system established in a controlled light environment for validation studies. In the interpretation of RGB values, Z-score (standardization) was utilized. The Z-score value is calculated using the formula $z = (X - \mu) / \sigma$. The Z-score is a numerical measure that describes the relationship between a value and the mean of a group of values [18].

In essence, the Z-score indicates how many standard deviations a data point is from the mean. Z-scores are measured in terms of standard deviations from the mean. A Z-score of 0 means the data point has the same score as the mean. Using this method, a different coefficient was obtained for each concentration for the resulting color, and concentration differentiations were achieved based on the obtained coefficient values. The variation of Z-Score values by concentration is shown in Figure 8.

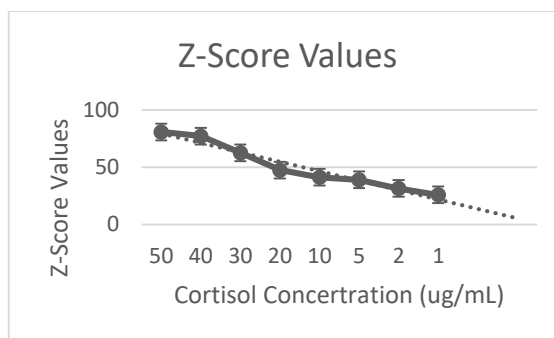


Figure 8 The graph showing the connection between cortisol concentrations and the Z-score coefficients resulting from validation studies.

The graph (Figure 8) illustrates the negative relationship between cortisol concentration ($\mu\text{g/mL}$) and Z-score values. As the cortisol concentration decreases from 50 $\mu\text{g/mL}$ to 1 $\mu\text{g/mL}$, the Z-score values correspondingly decrease from approximately 85 to 35. This inverse relationship indicates that higher cortisol concentrations result in higher Z-scores.

In this context, the Z-scores reflect the degree of color change detected by the microcontroller system. Higher cortisol concentrations induce more significant color changes, leading to higher Z-scores. Conversely, lower cortisol concentrations result in less intense color changes and lower Z-scores.

The error bars represent the standard deviation of the Z-score measurements for each cortisol concentration. Variability is higher at concentrations of 50 and 40 µg/mL, indicating some inconsistencies in measurements at these levels. In contrast, the error bars are smaller at lower across different concentrations highlight the system’s potential for real-time monitoring of cortisol levels, which is essential for stress management and the diagnosis of related disorders.

The high analytical performance is evidenced by the low detection limit (0.3 µg/mL) and the system’s ability to accurately measure cortisol concentrations within the range of 0.8 to 60 µg/mL. This graph substantiates the system’s sensitivity and reliability.

The graph (Figure 8) effectively illustrates the quantitative relationship between cortisol concentration and Z-score values obtained through colorimetric analysis facilitated by the ESP 32 microcontroller system. The decreasing Z-score values with decreasing cortisol concentrations validate the system’s sensitivity and reliability, confirming the potential of the developed wearable microfluidic device for continuous and accurate monitoring of cortisol levels in clinical and biomedical applications.

In validation studies, each sample was tested with 10 repetitions, and a standard cortisol curve was created (Figure 9).

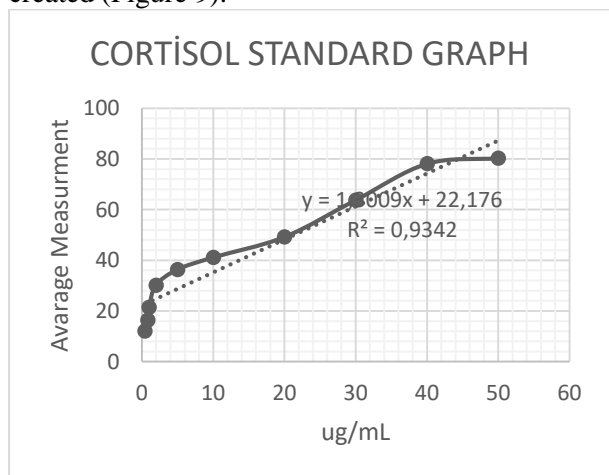


Figure 9 Standard graph showing cortisol concentration and label intervals.

The linear equation indicated on the graph (Figure 9), ($y = 1.3009x + 22.176$), shows that as cortisol concentration increases, the average measurement values also increase. This equation indicates that for each unit increase in cortisol, the average measurement increases by approximately

concentrations (5, 2, 1 µg/mL), suggesting more precise measurements at these levels.

The developed system demonstrates the capability to accurately measure cortisol levels across a wide range of concentrations. The consistency and predictability of Z-score values 1.3009 units, with a baseline measurement value of 22.176. The R^2 value of 0.9342, shown on the graph, indicates that the model fits the data well and has a strong explanatory power.

This graph (Figure 9) clearly demonstrates a linear relationship between cortisol concentration and average measurement values. The high R^2 value (0.9342) indicates that the linear model explains the data well and provides reliable results for measuring cortisol levels. This suggests that this standardization curve can be used for determining cortisol levels with high accuracy.

The ability to measure cortisol levels accurately and consistently is of great importance in both research and clinical applications. This graph (Figure 9) can serve as a reference for determining the cortisol concentrations in unknown samples, thereby enhancing the reliability of the results obtained. Consequently, this standard curve provides a valuable contribution to scientific studies and clinical applications by ensuring reliable and valid cortisol measurements.

In the scope of the study, slope, detection limit, and quantification limit values were calculated. The results are presented in Table 3.3.

Table 3.3: Table showing the validation results of cortisol RGB values.

Cortisol Validation Results	
Combined Standard Deviation	2,765629067
Inclination	212.332
Limit of Detection (LOD)	0,390749966
Limit of Quantification (LOQ)	1,172249898
Standard Curve Equation	$y = 21.233x + 3.3922$
R2 Value	$R^2 = 0.9439$

The determinable label range values are as shown in Table 3.4.

Table 3.4: The table showing the concentration values determinable by the created system.

Determined Label Intervals	
50	ug/mL
40	ug/mL
30	ug/mL
20	ug/mL
10	ug/mL
5	ug/mL
2	ug/mL
1	ug/mL
0,8	ug/mL

Table 3.5: Standard deviation, variance, relative standard deviation, and coefficient of variation values were examined for the correlation between samples for each ug/mL. Validation results conducted for 50, 40, 30, 20, 10, 5, 2, 1, 0.8 ug/mL, n=10, respectively.

50 ug/mL	
Standard Deviation (s)	0,662748834
Variance (s ²)	0,439236017
Relative Standard Deviation (RSD)	1,508867234
Coefficient of Variation	150,8867234
Label Interval	79.45733-81.64688
40 ug/mL	
Standard Deviation (s)	1,287411716
Variance (s ²)	1,657428926
Relative Standard Deviation (RSD)	0,776752291
Coefficient of Variation	77,67522912
Label Interval	74.996944-79.847878
30 ug/mL	
Standard Deviation (s)	2,058650398
Variance (s ²)	4,238041462
Relative Standard Deviation (RSD)	0,485755134
Coefficient of Variation	20,8182106
Label Interval	54.623752-70.617808
20 ug/mL	
Standard Deviation (s)	2,799559391
Variance (s ²)	7,837532784
Relative Standard Deviation (RSD)	0,357199066
Coefficient of Variation	35,71990661
Label Interval	43.147088- 52.271786
10 ug/mL	

Standard Deviation (s)	1,203181454
Variance (s ²)	1,447645611
Relative Standard Deviation (RSD)	0,831129832
Coefficient of Variation	83,11298323
Label Interval	38.410248-42.870638
5 ug/mL	
Standard Deviation (s)	2,24180767
Variance (s ²)	5,02570163
Relative Standard Deviation (RSD)	0,446068596
Coefficient of Variation	44,6068596
Label Interval	32.907808-39.867084
2 ug/mL	
Standard Deviation (s)	1,752836372
Variance (s ²)	3,072435346
Relative Standard Deviation (RSD)	0,570503908
Coefficient of Variation	57,0503908
Label Interval	26.93363-33.44529
1 ug/mL	
Standard Deviation (s)	2,826891729
Variance (s ²)	7,991316845
Relative Standard Deviation (RSD)	0,353745419
Coefficient of Variation	35,37454194
Label Interval	17.394198-25.924386
0.8 ug/mL	
Standard Deviation (s)	2,007717889
Variance (s ²)	4,030931121
Relative Standard Deviation (RSD)	0,498077945
Coefficient of Variation	49,80779449
Label Interval	13.186178-20.536012

4. Discussion and Conclusion

The research conducted in this study is examined in four main stages. In the first stage, a colorimetric reaction was performed using the blue tetrazolium method, where the color intensity increased proportionally with the concentration, shifting from transparent to magenta. A color change was observed at a concentration of 0.8 ng/mL, which was found to be suitable for human sweat samples as reported by Ethan Tu et al. (8/142 ng/mL) [14]. The color

intensity remained stable for up to one week as long as the Eppendorf tubes were not exposed to air. The blue tetrazolium method was repeated 10 times, and the colors obtained at specific cortisol concentrations were validated through RGB value readings.

In the second stage, various articles and designs aimed at the microfluidic layer were reviewed. Materials such as Whatman No. 4 paper and cotton-based absorbent pads, Whatman No. 1 chromatography paper, thin-layer chromatography paper, nitrocellulose membrane, and Whatman glass

microfiber filter paper were used. Studies were conducted to create the absorbent region, hydrophobization, and reaction area using these papers. Due to the different absorbency levels of each paper, varying amounts of reagent were applied to the reaction area. Cotton-based absorbent pads and Whatman glass microfiber filter paper were found to be more effective in reflecting color intensity. The difference in liquid retention between the two selected reaction areas affects the amount of sample collected and its transfer to the reaction region. Accordingly, a minimum of 50 μL sample was required to observe a visible color change in cotton-based absorbent pads, while 35 μL was determined for Whatman glass microfiber filter paper. These amounts were used in selecting the paper for the absorbent region and determining the flow in the microfluidic layer. The sizes of the Whatman No. 4 paper, cotton-based absorbent pads, Whatman No. 1 chromatography paper, thin-layer chromatography paper, Whatman glass microfiber filter paper, and coarse filter paper used were 1 cm^2 . Accordingly, coarse filter paper had the lowest liquid absorption capacity at 30 μL , while cotton-based absorbent pads had the highest at 50 μL . It was concluded that using cotton-based absorbent pads with the highest liquid absorption capacity would be efficient in sample collection from the user and transfer to the reaction area.

In hydrophobization performed using the thermoplastic method, the water contact angle was determined to be $90\pm 4^\circ$. Other hydrophobizing agents, such as paraffin, were not considered beneficial for wearable systems due to the potential for cracks during bending or stretching. Therefore, the use of the thermoplastic method for hydrophobization was deemed advantageous for the optimal use of the microfluidic layer. Despite being used in pharmaceutical coating and packaging and edible food packaging [15], no study was found in the literature regarding the hydrophobization of microfluidic layers using this method.

When the reaction areas were treated with solutions containing different concentrations of cortisol, the color intensity increased proportionally with the concentration. The study was repeated 10 times, and RGB intensities were determined by photographing with the ESP 32 CAM development board under constant light. Open-source software and hardware are crucial in the stages of scientific and commercial prototype development, being cost-effective and widely applicable. The ESP 32 CAM module, used in this study as one of the open-source development boards, although relatively new in

image-based processes, is expected to become more widespread due to its potential. In a 2020 study by Mingdian Liu et al., the ESP 32 CAM module was actively used as a camera module with data transfer features over Wi-Fi and Bluetooth [16]. However, the major disadvantage of the ESP 32 CAM module used in this study is the low resolution of its built-in camera hardware. Additionally, the built-in Wi-Fi module on the board experiences a drop in connection quality as it moves away from internet access points, requiring extra modules to overcome this issue. Extra efforts are needed to address these technical problems. Although colorimetric detection at lower concentrations and intermediate values is possible, limitations in colorimetric detection were encountered due to the camera features of the ESP 32 CAM module.

The obtained RGB values were evaluated with the standard score/Z-score from the images of the microfluidic layer captured with the ESP 32 CAM module. The obtained values were compared with the population mean through Z-scores. The correlation between cortisol concentration and Z-score values was proportional, as shown in the Z-score graph (Figure 9). Similarly, the relationship between the increase in cortisol concentration and the average Z-score values calculated for each concentration was shown in the cortisol standard graph (Figure 8).

The criteria evaluated for validation were conducted according to the instructions of Harris's Quantitative Chemical Analysis [17]. The combined standard deviation (σ), an estimated value of the population standard deviation (σ), was calculated. This value is the weighted average of the sample values. The practical detection limit is generally determined by multiplying the standard deviation of the signal measured for at least ten repeated solutions by three. To determine the detection limit, this value was divided by the slope of the proposed standard graph after being multiplied by three. This value was calculated as three times the detection limit [17]. The combined standard deviation was determined to be 0.028%. It shows a high degree of similarity in terms of statistical significance. The slope of the regression line, which indicates how much Y_i changes when the X_i variable changes by one unit, was calculated as 21.23. The significance of the unit varies between the label ranges determined within the system, namely 50, 40, 30, 20, 10, 5, 2, 1, 0.8 $\mu\text{g/mL}$. In addition, the concentration and Z-score ranges were evaluated internally. The lowest standard deviation and variance were calculated as 0.66-0.44 at 50 $\mu\text{g/mL}$ and 2.83-7.99 at 1 $\mu\text{g/mL}$, respectively. Therefore,

the confidence interval value was determined to be 50 µg/mL for the lowest concentration and 5 µg/mL for the highest concentration. When examining the label ranges, that is, the Z-score values, overlaps of 1.73 between 5 µg/mL and 10 µg/mL and 0.39 between 40 µg/mL and 50 µg/mL were observed.

This study has developed an innovative system enabling the rapid, accurate, and portable detection of cortisol using conventional image processing algorithms with the ESP 32 microcontroller and blue tetrazolium method. The system can accurately measure cortisol concentrations ranging from 0.8 to 60 µg/mL with a low detection limit of 0.3 µg/mL. Additionally, using thermoplastically hydrophobized microfluidic layers and cotton-based absorbent pads enhances the system's accuracy and reliability. This developed system offers a practical solution for non-invasive and real-time monitoring of cortisol levels, holding significant potential for clinical applications and personal health monitoring technologies.

The development of microfluidic layers in biotechnology studies and their use in health applications have become increasingly popular in recent years. One of the main reasons for this trend is the ability of technology applications to support minimal and more cost-effective systems that can replace large and high-cost devices. Our study aimed to create a system that strengthens this logic. Unlike high-cost systems like ELISA, which require long working hours and experienced personnel, our system is cost-effective, highly sensitive, and practical.

The potential of the developed system for real-time monitoring of cortisol levels provides significant insights for the diagnosis and management of stress-related disorders such as Cushing's syndrome and Addison's disease. The ability to non-invasively and continuously monitor

cortisol levels offers a practical solution for both clinical and personal health applications.

This research paves the way for further development of wearable microfluidic devices capable of monitoring various biomarkers, thereby contributing to personalized healthcare. The presented methodology and technology can be adapted for detecting other clinically relevant analytes, thus expanding the scope and impact of this research in the field of biosensors and wearable health technology.

In summary, this study offers a robust and innovative solution for cortisol monitoring, demonstrating the practical application of microcontroller and microfluidic technologies in biomedical engineering. The integration of these technologies enhances the feasibility and accuracy of continuous health monitoring, providing significant potential for future research and clinical applications.

Acknowledgment

This study was funded by Scientific Research Projects Coordination Unit of Istanbul University. Project number: FYL-2022-38254. It was also supported by the Istanbul Gedik University BAP Commission under the project number GDK202207-30.

Conflict of Interest Statement

There is no conflict of interest between the authors.

Statement of Research and Publication Ethics

The study is complied with research and publication ethics

References

- [1] S. Hiller-Sturmhöfel and A. Bartke, "The endocrine system: an overview," *Alcohol health and research world*, vol. 22, no. 3, pp. 153, 1998.
- [2] N. E. Muda, M. A. A. Bakar, and B. Y. Majlis, "The Use of Electronic Sensor in Hormone Analysis," *The Malaysian journal of medical sciences: MJMS*, vol. 6, no. 2, pp. 12, 1999.
- [3] S. Dalirirad and A. J. Steckl, "Aptamer-based lateral flow assay for point of care cortisol detection in sweat," *Sensors and Actuators B: Chemical*, vol. 283, pp. 79-86, 2019.
- [4] L. Lu, J. Zhang, Y. Xie, F. Gao, S. Xu, X. Wu, and Z. Ye, "Wearable health devices in health care: Narrative systematic review," *JMIR mHealth and uHealth*, vol. 8, no. 11, pp. e18907, 2020.
- [5] R. Royea, K. J. Buckman, M. Benardis, J. Holmes, R. L. Fletcher, E. Y. K. Ng, and J. D. Ellenhorn, "An introduction to the Cyncadia Breast Monitor: A wearable breast health monitoring device," *Computer methods and programs in biomedicine*, vol. 197, pp. 105758, 2020.

- [6] M. Rafiquzzaman, *Microcontroller Theory and Applications with the PIC18F*. John Wiley & Sons, 2018.
- [7] W. A. Stapleton, "Development Of A Library For Teaching And Implementing Resource-Limited Embedded Systems," in *Proceedings of the International Conference on Embedded Systems, Cyber-physical Systems, and Applications (ESCS)*, The Steering Committee of The World Congress in Computer Science, Computer Engineering and Applied Computing (WorldComp), 2011, pp. 1.
- [8] G. Gridling and B. Weiss, *Introduction to microcontrollers*, Vienna University of Technology Institute of Computer Engineering Embedded Computing Systems Group, 2007.
- [9] Y. Güven, E. Coşgun, S. Kocaoğlu, H. Gezici, and E. Yılmazlar, "Understanding the concept of microcontroller based systems to choose the best hardware for applications," 2017.
- [10] K. Hintz and D. Tabak, *Microcontrollers: architecture, implementation, and programming*. McGraw-Hill, Inc., 1992.
- [11] H. K. Kondaveeti, N. K. Kumaravelu, S. D. Vanambathina, S. E. Mathe, and S. Vappangi, "Computer Science Review," 2021.
- [12] R. Santos, "ESP32-CAM Take Photo and Display in Web Server," *randomnerdtutorials.com*, 2019. [Online]. Available: <https://randomnerdtutorials.com/>. [Accessed: 01-Jul-2022].
- [13] S. Santos, "ESP32-CAM Save Picture in Firebase Storage," *randomnerdtutorials.com*, 2022. [Online]. Available: <https://randomnerdtutorials.com/>. [Accessed: 18-Jul-2022].
- [14] E. Tu, P. Pearlmutter, M. Tiangco, G. Derose, L. Begdache, and A. Koh, "Comparison of colorimetric analyses to determine cortisol in human sweat," *ACS omega*, vol. 5, no. 14, pp. 8211-8218, 2020.
- [15] S. Bandyopadhyay, T. Saha, D. Sanétník, N. Saha, and P. Saha, "Thermo Compression of Thermoplastic Agar-Xanthan Gum-Carboxymethyl Cellulose Blend," *Polymers*, vol. 13, no. 20, pp. 3472, 2021.
- [16] M. Liu, Y. Zhao, H. Monshat, Z. Tang, Z. Wu, Q. Zhang, and M. Lu, "An IoT-enabled paper sensor platform for real-time analysis of isothermal nucleic acid amplification tests," *Biosensors and Bioelectronics*, vol. 169, pp. 112651, 2020.
- [17] D. C. Harris, *Quantitative Chemical Analysis*, W. H. Freeman, New York, 1995, pp. 750.